

THE ADHESION OF POLY(DIMETHYL SILOXANE) TO SILICA SUBSTRATES

THE ADHESION OF POLY(DIMETHYL SILOXANE) TO SILICA SUBSTRATES

BY LUNQUAN YU, B. ENG., M. ENG.

A Thesis Submitted to the School of Graduate Studies in Partial Fulfillment of the
Requirements for the Degree Master of Applied Science

McMaster University © Copyright by Lunquan Yu, June 2014

MASTER OF APPLIED SCIENCE (2014)
(Chemical Engineering)

McMaster University
Hamilton, Ontario

TITLE: The adhesion of poly(dimethyl siloxane) to silica substrates

AUTHOR: Lunquan Yu

B. Eng. (Sichuan University)

M. Eng. (Sichuan University)

SUPERVISOR: Professor Robert H. Pelton

NUMBER OF PAGES: xii, 40

Abstract

The adhesion of poly(dimethyl siloxane) (PDMS) to silica substrates was measured by 90 degree peel testing of PDMS strips cast on silica substrates. The objective of this work was to investigate the effects of silica surface chemistry on the adhesion between PDMS and silica substrate.

Silica substrates with different surface chemistry were prepared by both chemical modification and physical adsorption. Silane coupling agents were used to provide octyl chains and primary amino groups on the silica surfaces. Also silica surfaces were coated with cetyltrimethylammonium bromide (CTAB), polyvinylamine (PVAm) or poly(*N*-isopropylacrylamide) (PNIPAM) by physical adsorption. The adhesion samples were prepared by casting Sylgard[®] 184 silicone elastomers on silica surfaces followed by thermal curing.

Water contact angle measurements, scanning electron microscopy (SEM), X-ray photoelectron spectroscopy (XPS) and Fourier transform infrared microscopy (FTIR) were performed to measure the surface properties of the peel test samples. It is believed that hydrogen bonding between siloxane bonds in PDMS and silanol groups on silica substrate contributes to the strong adhesion of PDMS and silica surface. The adhesion forces significantly reduced by the adsorption of PVAm and PNIPAM onto silica surfaces. In addition, the introduction of primary amino groups on silica surface would poison the catalyst during the curing of PDMS, which causes the formation of low crosslinking PDMS

in the outer surface and is expected to decline the adhesion force. Lastly, the slightly reduce of adsorbed PVAm (340 kDa) on the silica substrate after peel test is considered to be useful for long-term lubrication.

Acknowledgements

First of all, I would like to express my deepest gratitude to my supervisor, Professor Robert H. Pelton, for his guidance, encouragement and assistance throughout my graduate study.

I would like to thank Prof. Emily Cranston for sharing knowledge on surface characterization and Prof. Michael Brook for useful discussion on PDMS curing process.

I would like to thank Dr. Danielle Covelli and Ms. Elna Luckham for their help to access the instruments in the Biointerfaces Institute, and Ms. Marcia Reid for SEM support in the Health Science Centre.

Moreover, I am grateful to all my friends at McMaster University, especially my colleagues in the McMaster Interfacial Technologies Group: Dr. Yuguo Cui, Dr. Songtao Yang, Roozbeh Mafi, Dr. Zuohe Wang, Zhuyuan Zhang, Zhen Hu, Dr. Jingyun Wang, Jieyi Liu, Dr. Shuxian Shi, Xiaofei Dong, Qiang Fu, Hajir Mokhtari, Sana Jahanshahi, Carla Abarca and Emil Gustafsson.

To Mr. Doug Keller and Ms. Sally Watson thank you for their Administrative work. Many thanks to Ms. Kathy Goodram, Ms. Lynn Falkiner, and Ms. Cathie Roberts for their administrative assistance, and also Ms. Lina Liu, Mr. Paul Gatt, Ms. Justyna Derkach and Mr. Dan Wright for their technical expertise support.

I acknowledge Alcon Laboratories and the Natural Sciences and Engineering Research Council of Canada for their financial support.

Lastly, I wish to express my gratitude to my family members for their endless love and support.

Table of Contents

Abstract	iii
Acknowledgements	v
Table of Contents	vii
List of Figures	ix
List of Tables	xi
Nomenclature	xii
Chapter 1 Introduction	1
1.1 Literature review	1
1.1.1 Adhesion mechanisms	1
1.1.2 Adhesion force measurements	3
1.1.3 Poly(dimethyl siloxane) silicone rubber	5
1.1.4 Surface modification of silica surface	7
1.2 Objectives	9
References	11
Chapter 2 Experimental Section	15
2.1 Materials	15
2.2 Experimental	15
2.2.1 Preparation of cleaned glass slides and quartz slides	15
2.2.2 Preparation of physical-adsorbed glass slides	16
2.2.3 Preparation of chemical-modified glass slides and quartz slides	16
2.2.4 Preparation of PDMS films adhered to glass slides (Glass/PDMS) and quartz (Quartz/PDMS)	17
2.2.5 90° Peel tests of PDMS films against glass slides and quartz slides	18
2.2.6 X-ray photoelectron spectroscopy (XPS)	19
2.2.7 Water contact angle measurements	20
2.2.8 Scanning electron microscopy (SEM)	20
2.2.9 Fourier transform infrared microscopy (FTIR)	20
References	21
Chapter 3 Results and Discussion	22

3.1	Results	22
3.2	Discussion	30
3.2.1	The effects of surface wettability of glass substrates on the adhesion behavior of PDMS	31
3.2.2	Adhesion behavior of PDMS against glass and quartz substrates	33
3.2.3	Adhesion behavior of PDMS against chemical-modified and physical-adsorbed glass substrate	35
3.2.4	The effects of molecular weight of absorbed PVAm on adhesion	36
3.3.5	The adhesion behavior of PDMS on recycled PVAm substrates	37
	References	38
Chapter 4	Conclusions	39

List of Figures

Figure 1. 1 Illustration of mechanical interlocking for adhesion between two substrates. .	1
Figure 1. 2 (a) Illustration of the setup of AFM; (b) Illustration of the measurement of force-distance curve.	4
Figure 1. 3 Typical force-displacement curve obtained from peel test.....	5
Figure 1. 4 Proposed mechanism of hydrosilylation reaction.....	6
Figure 1. 5 Proposed mechanism of platinum catalyzed hydrosilylation.	7
Figure 1. 6 Proposed reaction mechanism of silane coupling agent.	9
Figure 2. 1 Fabrication adhesion testing samples by casting Sylgard® 184 mixture in a mold.	18
Figure 2. 2 90° Peel test sample of PDMS film adhered to glass slide substrate.....	18
Figure 2. 3 Schematic illustration of 90° peel test for the adhesion sample with a 90° peel fixture.....	19
Figure 3. 1 Peel strengths of PDMS films against chemical-modified glass substrates from 90° peel tests. The peel tests were carried out with a 90° peel fixture and a crosshead rate of 50 mm/min at 23 °C and 50% RH. The error bars represent the standard deviation of the peel strength change of four replicates.	24
Figure 3. 2 Peel strengths of PDMS films against chemical-modified quartz substrates from 90° peel tests. The peel tests were carried out with a 90° peel fixture and a crosshead rate of 50 mm/min at 23 °C and 50% RH. The error bars represent the standard deviation of the peel strength change of four replicates.	24
Figure 3. 3 Peel strengths of PDMS films against physical-adsorbed glass substrates from 90° peel tests. The peel tests were carried out with a 90° peel fixture and a crosshead rate of 50 mm/min at 23 °C and 50% RH. The error bars represent the standard deviation of the peel strength change of four replicates.....	25
Figure 3. 4 Peel strengths of PDMS films against PVAm (340 kDa) adsorbed glass substrate and recycled PVAm (340 kDa) adsorbed glass substrate from 90° peel tests. The peel tests were carried out with a 90° peel fixture and a crosshead rate of 50 mm/min at 23 °C and 50% RH. The error bars represent the standard deviation of the peel strength change of four replicates.	26
Figure 3. 5 SEM images of different chemical-modified glass substrates after 90° peel test.	28
Figure 3. 6 Optical images of peeled substrate surfaces and pure Prh Glass surface as control.	29
Figure 3. 7 Surface ATR-FTIR spectra of different glass substrates after peel tests.....	30
Figure 3. 8 Illustration of proposed hydrogen bonding between PDMS and silica substrate.	31

Figure 3. 9 Comparison of peel strength and contact angle for chemical-modified glass substrates.....32

Figure 3. 10 Comparison of peel strength and contact angle for physical-adsorbed glass substrates.....33

Figure 3. 11 The ratio of relative oxygen and relative silicon concentration for Prh Glass and Prh Quartz substrates.....34

List of Tables

Table 3. 1 Summary of silica substrates in terms of sample names, treated agents and water contact angles.	22
Table 3. 2 Relative atomic concentration (%) of different glass substrate surfaces at 45° takeoff angle by XPS before and after PDMS peel tests.	27
Table 3. 3 Relative atomic concentration (%) of PVAm (340 kDa) adsorbed glass substrate surfaces at 45° takeoff angle by XPS before and after PDMS peel tests.	27

Nomenclature

AFM	Atomic force microscopy
ATR	Attenuated total reflection
CTAB	Cetyltrimethylammonium bromide
FTIR	Fourier transform infrared microscopy
μ CP	Microcontact printing
MEMS	Micro-electro-mechanical system
Mn	Number average molecular weight
Mw	Weight average molecular weight
PDMS	Poly(dimethyl siloxane)
PNIPAM	Poly(<i>N</i> -isopropylacrylamide)
Pt	Platinum
PVAm	Polyvinylamine
RH	Relative humidity
SEM	Scanning electron microscopy
XPS	X-ray photoelectron spectroscopy

Chapter 1 Introduction

1.1 Literature review

1.1.1 Adhesion mechanisms

Adhesion is involved between two surfaces in the form of intermolecular or/and interatomic interaction.^{1,2} Adhesion between adhesive and adherend contributes to the final properties of the adhesive system. There are four major mechanisms proposed to explain adhesion. However, no universal theory along can relate the adhesion phenomena in a comprehensive way.

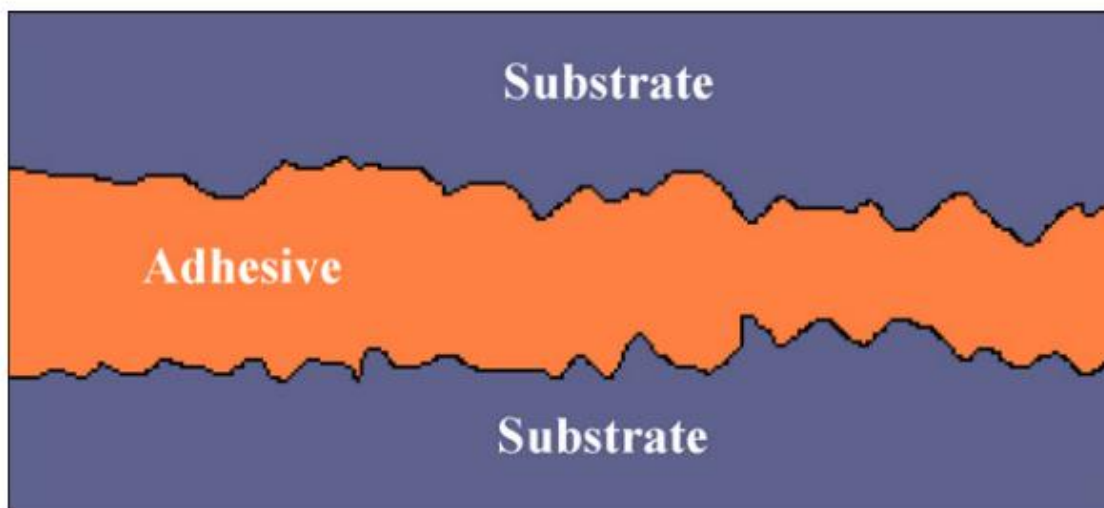


Figure 1. 1 Illustration of mechanical interlocking for adhesion between two substrates.

The mechanical interlocking theory was developed by McBain and Hopkins,³ which is applicable for irregular surface of the adherend. The adhesive is assumed to flow and fill the “micro-cavities” of the substrate and the adhesive joint formed mechanically after

curing.^{4 5} This theory is effective for rough or porous surfaces, such as paper, textile and wood.^{6,7} However, it can't be a major mechanism of adhesion for metallic surface.⁸

The diffusion theory was proposed by Voyutskii,⁹ describes adhesion between similar polymers, the core mechanism of which is referred to the mobility of the end-chain and chain-segment of polymers as well as their mutually solubility.¹⁰ This theory can well explain the reason why polymers with significant difference of solubility parameters are difficult to achieve good adhesion.

The electronic theory was developed by Derjaguin and Smilga, refers adhesion resulting from formation of electric double layer at the adhesive/adherend interface.¹¹ Electrostatic forces promote the creation of electric double layer, which is a result of the transfer of electrons from metal to adhesive.¹² The theory is more applicable for polymeric adhesive/metal substrate system.^{5, 13}

The adsorption theory is perhaps the most accepted theory of adhesion, which relates adhesion originating from atomic or molecular contact in the interface between adhesive and adherend where the attractive forces are developed. In general the interaction in the interface can be divided into two groups: primary bond and secondary bond (also referred as short range interaction and long range interaction). Metallic, ionic and covalent bonds formed chemisorption in the interface are referred as the primary bond, while acid-base interaction, van der Waals force and hydrogen bond formed physisorption in the interface

are referred as the secondary bond. Primary bonds are considered to have strong adhesive strength, whose interaction energy ranging from 15 to 250 kcal/mol are higher than those of secondary bonds less than 10 kcal/mol.^{5,8}

1.1.2 Adhesion force measurements

Measuring the adhesion force between two objects is usually performed to evaluate the adhesion behaviour. Among some of the techniques used to study the adhesion force atomic force microscopy (AFM) and peel test are two applicable techniques to measure the adhesion force in the nanoscale and the macroscale, respectively.

AFM is useful to study the surface force with the force-distance curve measurement, which is illustrated in **Figure 1.2**.^{14, 15} However, there were problems when comparing the obtained curves with the theoretical models due to the poorly defined geometry of AFM tip.¹⁶ The colloidal probe AFM is a powerful method to measure the surface which was developed by Ducker and Butt over 20 years ago.^{16, 17, 18} The colloidal probe is usually prepared by attaching spherical particle with well defined geometry to an AFM cantilever.

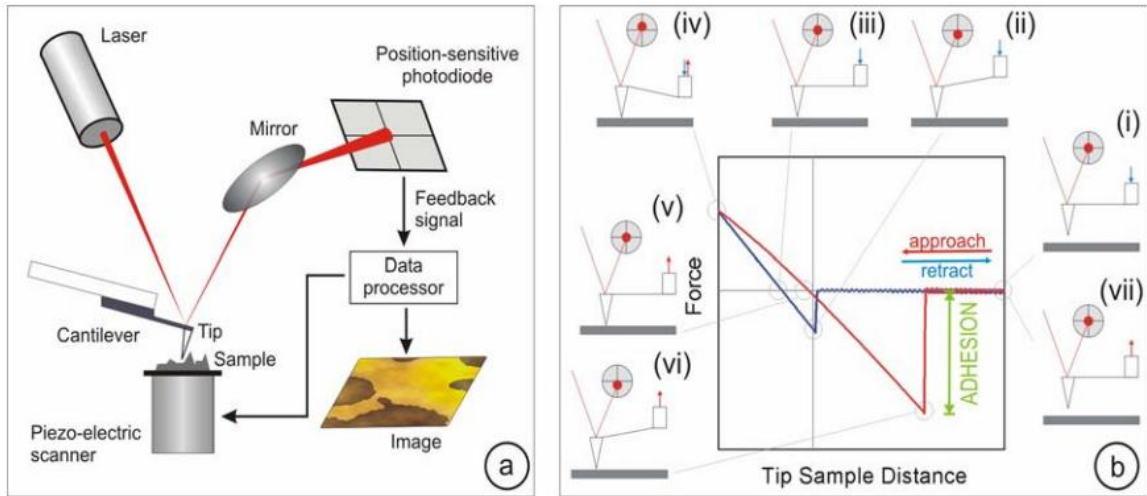


Figure 1. 2 (a) Illustration of the setup of AFM; **(b)** Illustration of the measurement of force-distance curve.¹⁵

The peel test is a common method for direct adhesion measurement.¹ It is a destructive method to measure the delamination force at the interface. Peel tests give qualitative data in terms of peel strength, which provides a quantitative measurement for adhesion. Peel strength is not a physical property for the adhesion but a relative value, which strongly dependent on the testing methods and operating conditions.¹

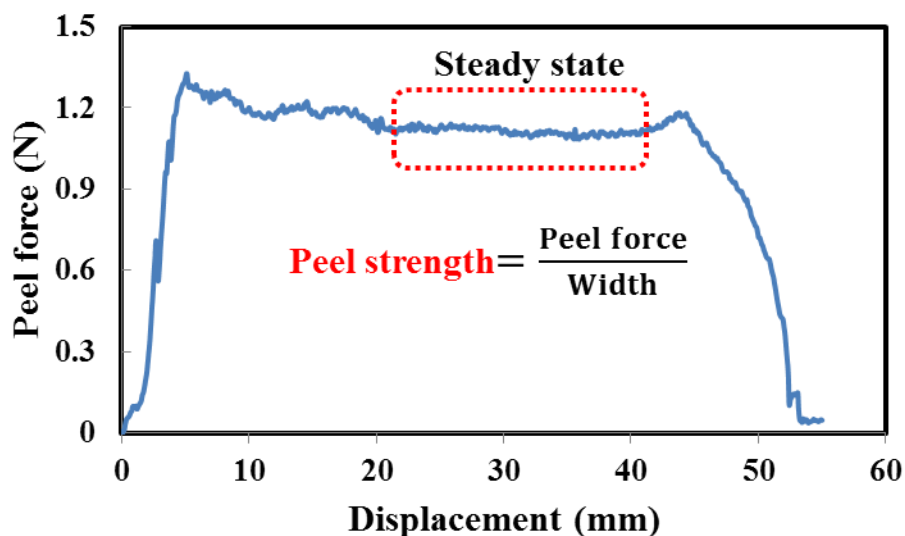


Figure 1.3 Typical force-displacement curve obtained from peel test.

In the peel test samples are peeled off substrates and the forces required to delaminate the sample from their backing materials are recorded.^{19, 20} In a typical peel test, adhesive tape is first placed by pressing on the substrate surface. Then one end of the tape is fixed at a constant angle of pull. Either constant peel force or constant peel rate is used to carry out the peel test. Lastly the peel strength is calculated by averaging the peel force in the steady state over the width of the specimen (**Figure 1.3**).

1.1.3 Poly(dimethyl siloxane) silicone rubber

Poly(dimethyl siloxane) (PDMS) is one of the most popular materials for polymer based fabrications, such as microfluidic devices,^{21, 22, 23, 24, 25, 26} microcontact printing (μCP)^{27, 28, 29, 30, 31} and bio-MEMS (micro-electro-mechanical system).^{32, 33, 34, 35, 36} The wide applications of PDMS contribute to its numerous excellent features, including low manufacturing cost, biocompatibility, elastic properties, and reliable microfabrication

procedure.^{37, 38, 39} PDMS is known as silicone rubber, which is a frequently used polymeric organosilicon compounds. The most widely used flexible PDMS for microfluidic applications is prepared with a commercial Dow Corning Sylgard[®] 184 silicone elastomer kit, which consists two-part liquid components. PDMS rubber is usually obtained by simply mixing Sylgard[®] 184 silicone elastomer base with curing agent in a 10:1 ratio by weight followed by thermal curing for a few hours.^{40, 41}

It is widely accepted that the crosslinked PDMS is cured by an organometallic addition reaction. The siloxane base consists of vinyl terminated oligomers and the crosslinkable oligomers are comprised of at least three silicon hydride (Si-H) bonds per polymer chain. The addition reaction is catalyzed by a platinum-based catalyst (e.g. Karstedt's catalyst or H_2PtCl_6) in the curing agent through a hydrosilylation mechanism to form new Si-C bonds from Si-H bonds and vinyl groups in the oligomers (**Figure 1.4** and **Figure 1.5**). The crosslinking network of PDMS is contributed to the multiple reaction sites on siloxane base and crosslinkable oligomers.^{42, 43}

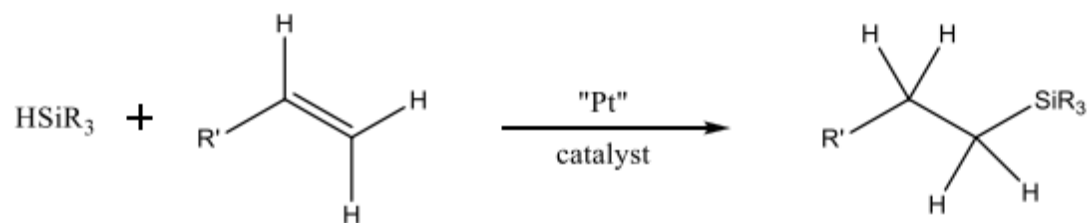


Figure 1. 4 Proposed mechanism of hydrosilylation reaction.⁴²

The platinum based catalyst can be poisoned by amine containing compounds, which cause inhibition of the PDMS curing process and thus affect the overall properties of the final PDMS.^{42, 43, 44, 45}

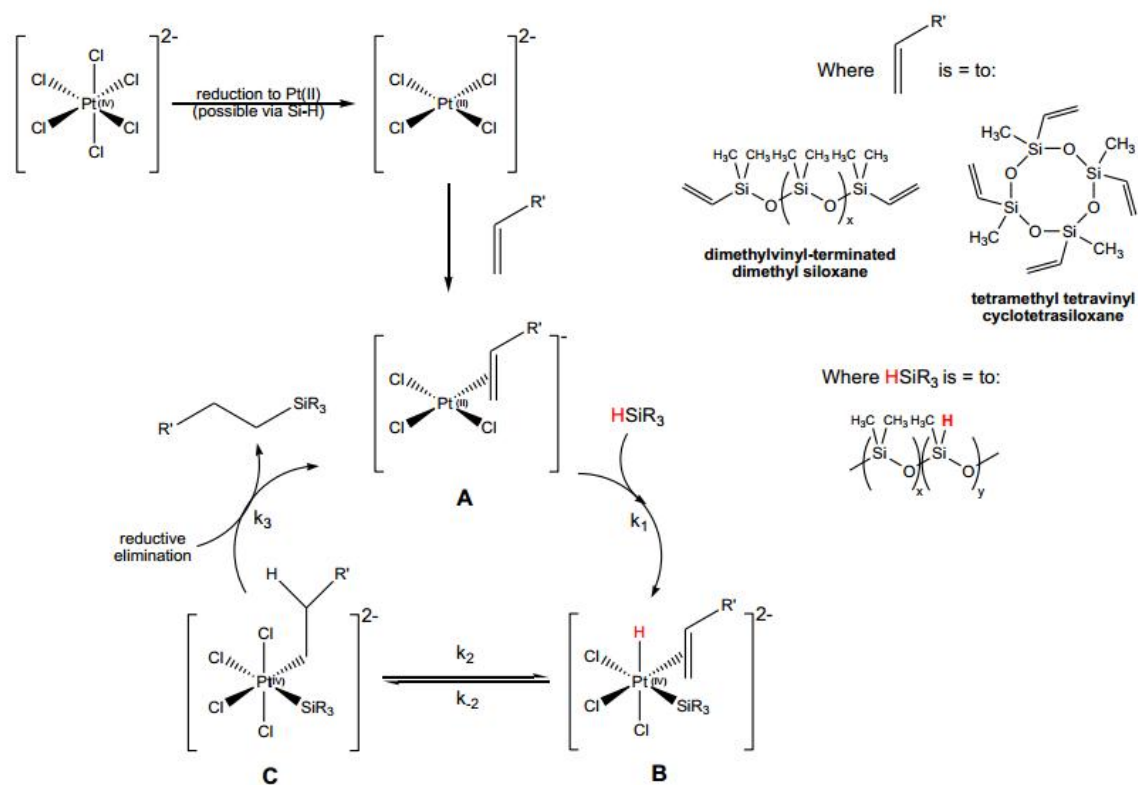


Figure 1. 5 Proposed mechanism of platinum catalyzed hydrosilylation.⁴²

1.1.4 Surface modification of silica surface

Silicate materials are widely used as solid substrates due to their significantly lower cost and versatility. Surface treatments with foreign reagents are commonly applied to obtain diverse surface chemistry for the outer silica surface while retaining the substrate geometry as well as mechanical properties. In general there are two major techniques used to perform the surface treatment: physisorption technique and chemisorption technique.

Silica surface is generally covered with silanol groups and thus considered to be negative charge, which render the surface tending to adsorb electron deficient species.⁴⁶ Surfactants or amphiphilic polymers are usually used to modify silica surface by physical adsorption. The driving force in the process of physisorption is electrostatic interaction or hydrogen bonding.

Compared with physisorption chemisorption through covalent attachment provides with much stronger interaction between adsorbent and silica substrates. The surface modification can be carried out by either using silane coupling agents or grafting with polymers. Silane coupling agents are most widely used compound with small molecule weight. Their represented structure appears as $\text{RSi}(\text{OX})_3$ or RSiCl_3 where R is the organic functional group and X is the hydrolysable group (e.g. methyl or ethyl group)^{47, 48, 49}. The R group can be either alkyl group for polymerization or other functional groups (e.g. amino group).^{50, 51, 52} The reaction mechanism of silane coupling agent is illustrated in **Figure 1.6**. The reactive silicon hydride (Si-H) undergo hydrolysis reaction with water molecule to form reactive silanol groups (Si-OH), then silanol group are chemically bonded to the silica surface through dehydration condensation. Also silane coupling agents are usually used as adhesion promoter in industry applications.⁵³

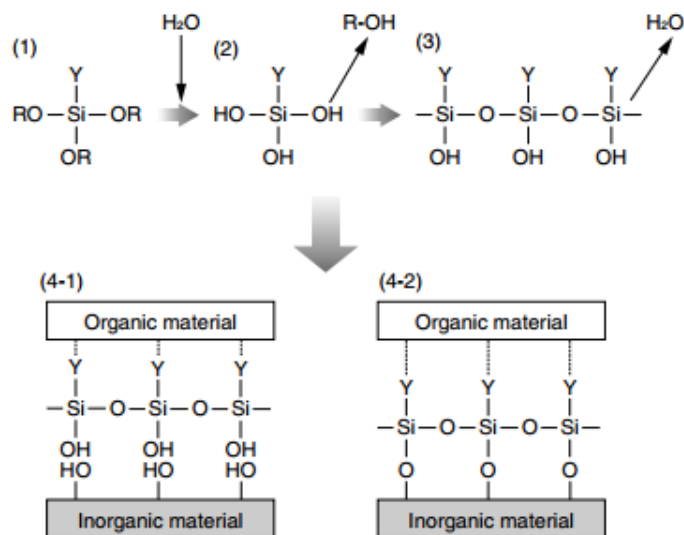


Figure 1. 6 Proposed reaction mechanism of silane coupling agent.⁵⁴

1.2 Objectives

Our industry partner Alcon has a demolding problem when they release the silicone hydrogel contact lens from the silicate molds after the curing process, which is harmful for their continuous manufacturing and increases the cost. In this work I used PDMS as a model materials. For one reason is that silicone is one of the major components of the silicone hydrogel contact lens. Also PDMS is used to develop the adhesion test. And silicate substrates, such as glass and quartz, were selected as adherend. Physical adsorption and chemical modification were carried out to obtain diverse surface chemistry for the silica substrates. A direct peel testing was applied to investigate the adhesion properties of PDMS on silica surface with different surface chemistry.

The overall objective of this project is to develop simple methods to predict the adhesion between PDMS silicone rubber and silica substrates. The specific objectives are listed below:

1. To prepare a series of silica substrates with varying surface chemistry by either physisorption of surfactant and water-soluble polymers or chemisorption of silane coupling agents.
2. To measure the adhesion force between PDMS silicone rubber and treated silica substrates using a 90° peel test.
3. To investigate the effects of the surface chemistry of silica substrate on the overall adhesion behavior.

References

1. Awaja, F.; Gilbert, M.; Kelly, G.; Fox, B.; Pigram, P. J., Adhesion of polymers. *Progress in polymer science* **2009**, *34* (9), 948-968.
2. Poisson, C.; Hervais, V.; Lacrampe, M.; Krawczak, P., Optimization of PE/binder/PA extrusion blow-molded films. II. Adhesion properties improvement using binder/EVA blends. *Journal of applied polymer science* **2006**, *101* (1), 118-127.
3. McBain, J.; Hopkins, D., On adhesives and adhesive action. *The Journal of Physical Chemistry* **1925**, *29* (2), 188-204.
4. Schultz, J.; Nardin, M.; Pizzi, A.; Mittal, K., Handbook of adhesive technology. *Marcel and Dekker, New York* **1994**.
5. Kinloch, A. J., *Adhesion and adhesives: science and technology*. Springer: 1987.
6. Kinloch, A., The science of adhesion. *Journal of materials science* **1980**, *15* (9), 2141-2166.
7. Fourche, G., An overview of the basic aspects of polymer adhesion. Part I: Fundamentals. *Polymer Engineering & Science* **1995**, *35* (12), 957-967.
8. Semoto, T.; Tsuji, Y.; Yoshizawa, K., Molecular Understanding of the Adhesive Force between a Metal Oxide Surface and an Epoxy Resin. *The Journal of Physical Chemistry C* **2011**, *115* (23), 11701-11708.
9. Voyutskii, S., Some comments on the series of papers “interfacial contact and bonding in autohesion”. *The Journal of Adhesion* **1971**, *3* (1), 69-76.
10. Wake, W. C., Adhesion and the Formulation of Adhesives. **1976**.
11. Derjaguin, B.; Smilga, V., Electronic theory of adhesion. *Journal of Applied Physics* **2004**, *38* (12), 4609-4616.
12. Von Harrach, H. G.; Chapman, B., Charge effects in thin film adhesion. *Thin Solid Films* **1972**, *13* (1), 157-161.
13. Hiemenz, P. C.; Rajagopalan, R., *Principles of Colloid and Surface Chemistry, revised and expanded*. CRC Press: 1997; Vol. 14.
14. Cappella, B.; Dietler, G., Force-distance curves by atomic force microscopy. *Surface science reports* **1999**, *34* (1), 1-104.
15. Stegemann, B.; Backhaus, H.; Kloss, H.; Santner, E., Spherical AFM probes for adhesion force measurements on metal single crystals. *Modern Research and Educational Topics in Microscopy, Series* **2007**, *3*, 820-827.
16. Kappl, M.; Butt, H. J., The colloidal probe technique and its application to adhesion force measurements. *Particle & Particle Systems Characterization* **2002**, *19* (3), 129-143.
17. Ducker, W. A.; Senden, T. J.; Pashley, R. M., Direct measurement of colloidal forces using an atomic force microscope. *Nature* **1991**, *353* (6341), 239-241.
18. Ducker, W. A.; Senden, T. J.; Pashley, R. M., Measurement of forces in liquids using a force microscope. *Langmuir* **1992**, *8* (7), 1831-1836.
19. Miller, J. A.; Von Jakusch, E. A., Pressure-sensitive adhesive composition, tape and diaper closure system. Google Patents: 1991.

20. Li, L.; Tirrell, M.; Korba, G. A.; Pocius, A. V., Surface energy and adhesion studies on acrylic pressure sensitive adhesives. *The Journal of Adhesion* **2001**, *76* (4), 307-334.
21. Leclerc, E.; Sakai, Y.; Fujii, T., Microfluidic PDMS (polydimethylsiloxane) bioreactor for large-scale culture of hepatocytes. *Biotechnology progress* **2004**, *20* (3), 750-755.
22. Rhee, S. W.; Taylor, A. M.; Tu, C. H.; Cribbs, D. H.; Cotman, C. W.; Jeon, N. L., Patterned cell culture inside microfluidic devices. *Lab on a Chip* **2005**, *5* (1), 102-107.
23. Anderson, J. R.; Chiu, D. T.; Jackman, R. J.; Cherniavskaya, O.; McDonald, J. C.; Wu, H.; Whitesides, S. H.; Whitesides, G. M., Fabrication of topologically complex three-dimensional microfluidic systems in PDMS by rapid prototyping. *Analytical Chemistry* **2000**, *72* (14), 3158-3164.
24. Toepke, M. W.; Beebe, D. J., PDMS absorption of small molecules and consequences in microfluidic applications. *Lab Chip* **2006**, *6* (12), 1484-1486.
25. Tan, F.; Leung, P. H.; Liu, Z.-b.; Zhang, Y.; Xiao, L.; Ye, W.; Zhang, X.; Yi, L.; Yang, M., A PDMS microfluidic impedance immunosensor for *E. coli* O157: H7 and *Staphylococcus aureus* detection via antibody-immobilized nanoporous membrane. *Sensors and Actuators B: Chemical* **2011**, *159* (1), 328-335.
26. Devaraju, N. S. G. K.; Unger, M. A., Pressure driven digital logic in PDMS based microfluidic devices fabricated by multilayer soft lithography. *Lab on a Chip* **2012**, *12* (22), 4809-4815.
27. Kaufmann, T.; Ravoo, B. J., Stamps, inks and substrates: polymers in microcontact printing. *Polymer Chemistry* **2010**, *1* (4), 371-387.
28. Wendeln, C.; Ravoo, B. J., Surface patterning by microcontact chemistry. *Langmuir* **2012**, *28* (13), 5527-5538.
29. Zhou, X.; Boey, F.; Huo, F.; Huang, L.; Zhang, H., Chemically functionalized surface patterning. *Small* **2011**, *7* (16), 2273-2289.
30. Kaufmann, T.; Gokmen, M. T.; Wendeln, C.; Schneiders, M.; Rinnen, S.; Arlinghaus, H. F.; Bon, S. A.; Du Prez, F. E.; Ravoo, B. J., "Sandwich" microcontact printing as a mild route towards monodisperse janus particles with tailored bifunctionality. *Advanced Materials* **2011**, *23* (1), 79-83.
31. Liao, W.-S.; Cheunkar, S.; Cao, H. H.; Bednar, H. R.; Weiss, P. S.; Andrews, A. M., Subtractive patterning via chemical lift-off lithography. *Science* **2012**, *337* (6101), 1517-1521.
32. Bashir, R., BioMEMS: state-of-the-art in detection, opportunities and prospects. *Advanced drug delivery reviews* **2004**, *56* (11), 1565-1586.
33. Velten, T.; Ruf, H. H.; Barrow, D.; Aspragathos, N.; Lazarou, P.; Jung, E.; Malek, C. K.; Richter, M.; Kruckow, J.; Wackerle, M., Packaging of bio-MEMS: strategies, technologies, and applications. *Advanced Packaging, IEEE Transactions on* **2005**, *28* (4), 533-546.
34. Zagnoni, M., Miniaturised technologies for the development of artificial lipid bilayer systems. *Lab on a Chip* **2012**, *12* (6), 1026-1039.

35. Mata, A.; Fleischman, A. J.; Roy, S., Characterization of polydimethylsiloxane (PDMS) properties for biomedical micro/nanosystems. *Biomedical microdevices* **2005**, *7* (4), 281-293.
36. Ziaie, B.; Baldi, A.; Lei, M.; Gu, Y.; Siegel, R. A., Hard and soft micromachining for BioMEMS: review of techniques and examples of applications in microfluidics and drug delivery. *Advanced drug delivery reviews* **2004**, *56* (2), 145-172.
37. Whitesides, G. M., The origins and the future of microfluidics. *Nature* **2006**, *442* (7101), 368-373.
38. Sia, S. K.; Whitesides, G. M., Microfluidic devices fabricated in poly (dimethylsiloxane) for biological studies. *Electrophoresis* **2003**, *24* (21), 3563-3576.
39. Anderson, J. R.; Chiu, D. T.; Wu, H.; Schueller, O. J.; Whitesides, G. M., Fabrication of microfluidic systems in poly (dimethylsiloxane). *Electrophoresis* **2000**, *21*, 27-40.
40. Qin, D.; Xia, Y.; Whitesides, G. M., Soft lithography for micro-and nanoscale patterning. *Nature protocols* **2010**, *5* (3), 491-502.
41. Wilbur, J. L.; Kumar, A.; Kim, E.; Whitesides, G. M., Microfabrication by microcontact printing of self-assembled monolayers. *Advanced Materials* **1994**, *6* (7-8), 600-604.
42. Ortiz-Acosta, D. *Sylgard® Cure Inhibition Characterization*; Los Alamos National Laboratory (LANL): 2012.
43. Brook, M. A., *Organosilicon Chemistry: Synthetic Applications in Organic, Organometallic, Materials, and Polymer Chemistry*. J. Wiley: 1999.
44. Heyries, K. A.; Marquette, C. A.; Blum, L. J., Straightforward protein immobilization on Sylgard 184 PDMS microarray surface. *Langmuir* **2007**, *23* (8), 4523-4527.
45. Kishi, K.; Ishimaru, T.; Ozono, M.; Tomita, I.; Endo, T., Development and application of a latent hydrosilylation catalyst. IX. Control of the catalytic activity of a platinum catalyst by polymers bearing amine moieties. *Journal of Polymer Science Part A: Polymer Chemistry* **2000**, *38* (5), 804-809.
46. Parida, S. K.; Dash, S.; Patel, S.; Mishra, B., Adsorption of organic molecules on silica surface. *Advances in Colloid and Interface Science* **2006**, *121* (1), 77-110.
47. Plueddemann, E. P., *Silane coupling agents*. Springer: 1982.
48. Kaas, R.; Kardos, J., The interaction of alkoxy silane coupling agents with silica surfaces. *Polymer Engineering & Science* **1971**, *11* (1), 11-18.
49. Xie, Y.; Hill, C. A.; Xiao, Z.; Militz, H.; Mai, C., Silane coupling agents used for natural fiber/polymer composites: A review. *Composites Part A: Applied Science and Manufacturing* **2010**, *41* (7), 806-819.
50. Wang, N.; Guo, Y.; Xu, H.; Liu, X.; Zhang, L.; Qu, X.; Zhang, L., Preparation of a silica/poly (n-butyl acrylate-co-acrylic acid) composite latex and its pressure-sensitive properties. *Journal of applied polymer science* **2009**, *113* (5), 3113-3124.
51. Tamai, T.; Watanabe, M., Acrylic polymer/silica hybrids prepared by emulsifier-free emulsion polymerization and the sol-gel process. *Journal of Polymer Science Part A: Polymer Chemistry* **2006**, *44* (1), 273-280.

52. Althues, H.; Henle, J.; Kaskel, S., Functional inorganic nanofillers for transparent polymers. *Chemical Society Reviews* **2007**, *36* (9), 1454-1465.
53. Plueddemann, E. P., Nature of Adhesion Through Silane Coupling Agents. In *Silane Coupling Agents*, Springer: 1991; pp 115-152.
54. Miyatake, K.; Ohama, O.; Kawahara, Y.; Urano, A.; Kimura, A., Study on Analysis Method for Reaction of Silane Coupling Agent on Inorganic Materials. *SEI TECHNICAL REVIEW-ENGLISH EDITION*- **2007**, *65*, 21.

Chapter 2 Experimental Section

2.1 Materials

Deionized water ($18.2 \text{ M}\Omega \text{ cm}^{-1}$) was purified from a Millipore system (Thermo Scientific, Asheville, NC). The glass slides ($75.0 \text{ mm} \times 25.0 \text{ mm}$, thickness 0.96 to 1.06 mm) and quartz microscope slides ($76.2 \text{ mm} \times 25.4 \text{ mm}$, thickness 1 mm) were obtained from Corning and Ted Pella, respectively. Sylgard[®] 184 silicone elastomer kit was purchased from Dow Corning (Midland, MI). Three types of polyvinylamine (PVAm) with different molecular weights, LUPAMIN[®] 1595 (10 kDa), LUPAMIN[®] 5095 (45 kDa) and LUPAMIN[®] 9095 (340 kDa) were gifts from BASF (Ludwigshafen, Germany). The PVAm samples were purified by dialysis against deionized water and freeze dried. The degrees of hydrolysis of the treated PVAm were about 73%, 75% and 91%, respectively.¹ Cetyltrimethylammonium bromide (CTAB) (Sigma), toluene (Sigma-Aldrich), dehydrated alcohol, acetone (Sigma-Aldrich), triethoxyoctyl silane (Aldrich), ¹H, ¹H, ²H, ²H-perfluorooctyltriethoxysilane (Aldrich), (3-aminopropyl)trimethoxysilane (Aldrich), poly(*N*-isopropylacrylamide) (PNIPAM) ($M_v:39000$, $M_w/M_n:1.45$) (Polymer Source) and amino terminated poly(*N*-isopropylacrylamide) (NH₂-PNIPAM) ($M_n:7110$, $M_w/M_n:1.26$) (Polymer Source) were used as received from their respective suppliers.

2.2 Experimental

2.2.1 Preparation of cleaned glass slides and quartz slides

The preparation of cleaned glass slides and quartz slides were carried out with a modified method as refereces^{2,3}. The glass slides were sonicated in deionized water for 30 min and

then dried in nitrogen flow following by heating in the oven at 100 °C for 30 min. Then the dried glass slides were sonicated in acetone for 30 min, and dried with nitrogen flow and in the oven at 100 °C for 30 min. The prepared glass slides were denoted as “Glass” slides.

The dry glass slides were cleaned by soaking in fresh piranha solution (H_2SO_4 : H_2O_2 : 70% : 30% wt%) for 2 h. Then they were rinsed sequentially with deionized water and dehydrated ethanol, and dried with nitrogen flow and then in the oven at 100 °C for 60 min.^{2, 3} The obtained glass slides were denoted as “Prh Glass” slides. “Quartz” slides and “Prh Quartz” slides were prepared following the same protocols mentioned above. The water contact angles on the treated glass slides and quartz slides were all around 5°.

2.2.2 Preparation of physical-adsorbed glass slides

The cleaned Prh Glass slides were soaked in CTAB (0.2 wt%), PVAm (10 kDa, 45 kDa and 340 kDa) (0.5 wt%), PNIPAM (0.5wt%) and NH₂-PNIPAM (0.5wt%) solutions to allow the adsorption of surfactant and polymers to glass surfaces overnight at room temperature, respectively. Then the glass slides were rinsed with deionized water, dried with nitrogen flow and heated in the oven at 100 °C for 30 min.

The treated glass slides were denoted as “CTAB Glass”, “PVAm (10 kDa) Glass”, “PVAm (45 kDa) Glass”, “PVAm (340 kDa) Glass”, “PNIPAM Glass” and “NH₂-PNIPAM Glass”, respectively.

2.2.3 Preparation of chemical-modified glass slides and quartz slides

The cleaned Prh Glass slides were soaked in triethoxy(octyl) silane (5 wt%), (3-aminopropyl)trimethoxysilane (5 wt%) and ^1H , ^1H , ^2H , ^2H -perfluorooctyltriethoxysilane (3 wt%) toluene solutions overnight, respectively. Then the glass slides were rinsed sequentially with toluene and acetone, and dried with nitrogen flow and in the oven at 100 °C for 30 min.

The obtained glass slides were denoted as “C8 Glass” and “NH2 Glass”, respectively. C8 Quartz and NH2 Quartz slides were prepared with the same method above using Prh Quartz.

2.2.4 Preparation of PDMS films adhered to glass slides (Glass/PDMS) and quartz (Quartz/PDMS)

Adhesion testing samples were fabricated by casting a mixture of Sylgard[®] 184 silicone elastomer kit against glass slide substrates in a mold (**Figure 2.1**). The base resin and curing agent of Sylgard 184 were mixed in a mass ratio of 10 : 1 and degassed in vacuum until the disappearance of bubbles. Then the mixture was poured into the mold and cured at 100 °C for 3 h. The PDMS samples were obtained with a dimension of 65.0 mm × 18.0 mm × 0.2 mm (length × width × thickness) (**Figure 2.2**).

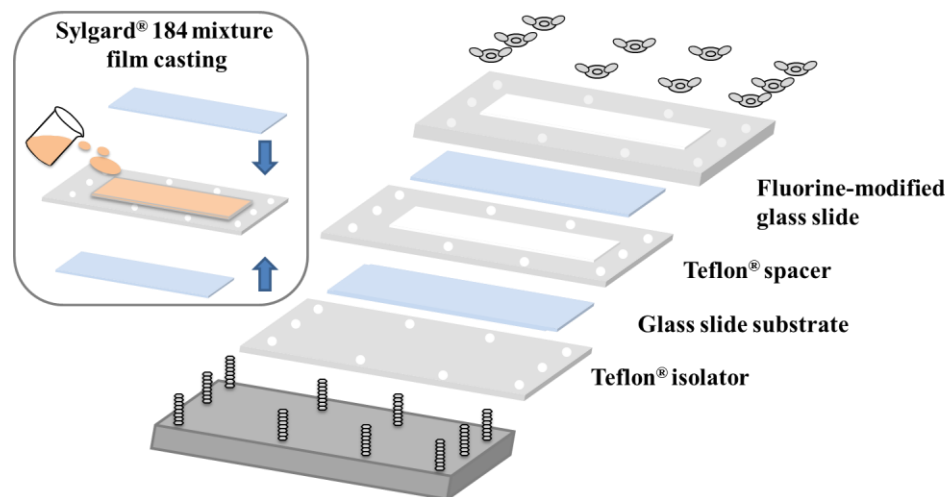


Figure 2. 1 Fabrication adhesion testing samples by casting Sylgard® 184 mixture in a mold.

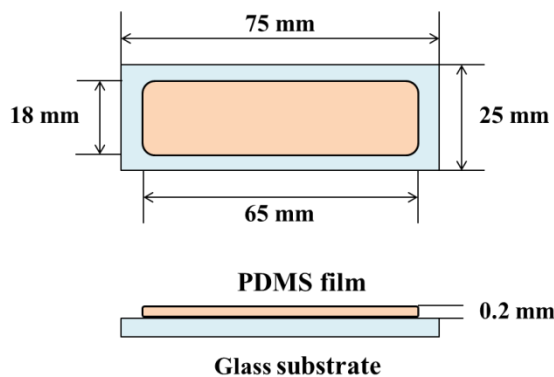


Figure 2. 2 90° Peel test sample of PDMS film adhered to glass slide substrate.

2.2.5 90° Peel tests of PDMS films against glass slides and quartz slides

The peel tests of PDMS films against glass slide substrates and quartz slide substrates were carried out by an Instron 4411 universal testing system (Instron Corp., Norwood, MA) with a 90° peel fixture and at a crosshead rate of 50 mm/min at 23 °C and 50% RH. About 10 mm of the film on one end was carefully peeled off the substrate and fixed with a screw

grip before the peel test (**Figure 2.3**). The data were recorded as peel force versus displacement. Four replicates were tested for each sample.

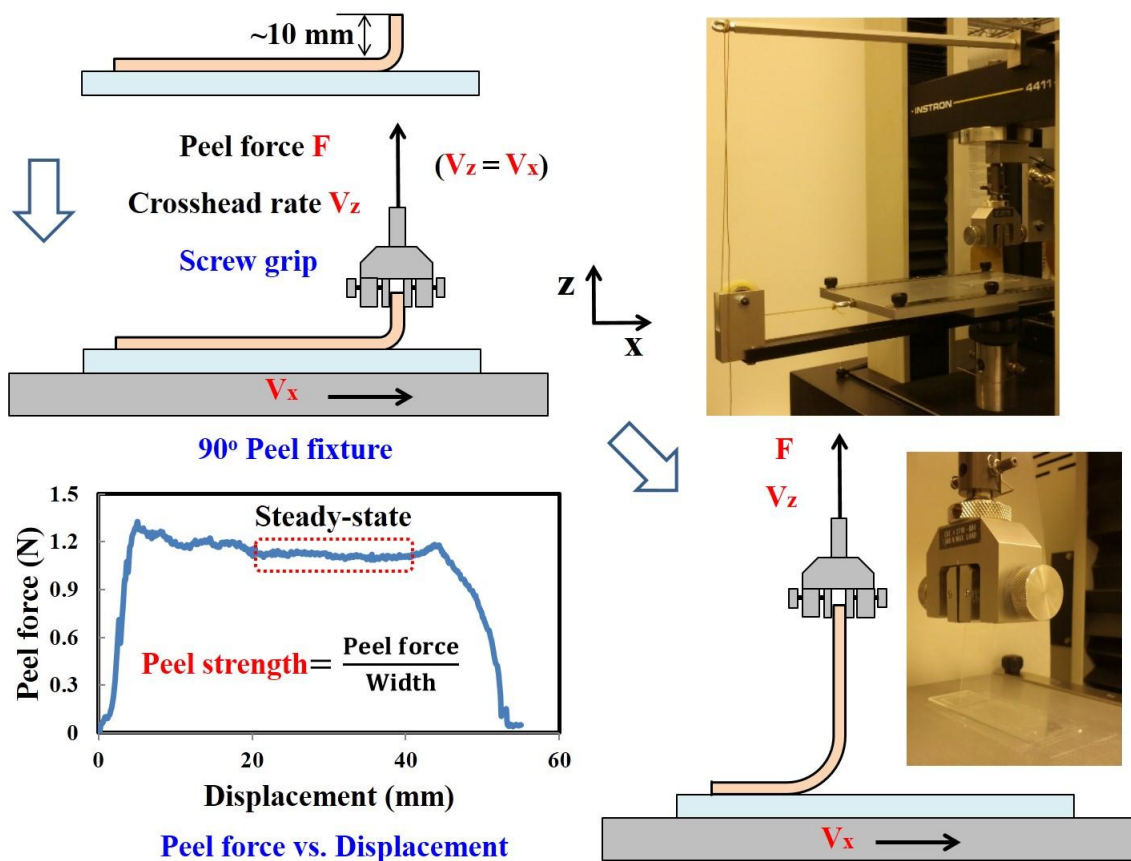


Figure 2. 3 Schematic illustration of 90° peel test for the adhesion sample with a 90° peel fixture.

2.2.6 X-ray photoelectron spectroscopy (XPS)

X-ray photoelectron spectra were recorded on a PHI Quantera II imaging and scanning X-ray photoelectron spectrometer (Physical Electronics, MN). Sample surfaces were radiated with a source of monochromatized Al $K\alpha$ (280 eV) with a 45° takeoff angle, a 200 μm beam size and a 50 W power. For each measurement five sweeps were performed.

2.2.7 Water contact angle measurements

The water contact angle measurements of the sample surfaces were performed by the sessile-drop technique using a Krüss DSA contact angle apparatus at room temperature. The mean contact angles were recorded on sample surfaces at room temperature; all droplets were about 20 μm in volume. Four replicates were tested for each sample.

2.2.8 Scanning electron microscopy (SEM)

Sample surfaces were coated with gold layer with a SEM coating unit E5100 (Polaron instruments Inc.). Surface images were examined by scanning electron microscopy with a VEGA\\LSU SEM (Tescan, Czech Republic) at an operating voltage of 5 kV.

2.2.9 Fourier transform infrared microscopy (FTIR)

FTIR imaging and single point spectroscopy of the sample surfaces were obtained using a Bruker Hyperion 3000 microscope fitted with an attenuated total reflection (ATR) objective and coupled with a Bruker Vertex 70 FTIR.

References

1. Wen, Q.; Vincelli, A. M.; Pelton, R., Cationic polyvinylamine binding to anionic microgels yields kinetically controlled structures. *Journal of colloid and interface science* 2012, 369 (1), 223-230.
2. Zhang, Z.; Hu, R.; Liu, Z., Formation of a porphyrin monolayer film by axial ligation of protoporphyrin IX zinc to an amino-terminated silanized glass surface. *Langmuir* 2000, 16 (3), 1158-1162.
3. Twardowski, M.; Nuzzo, R. G., Chemically mediated grain growth in nanotextured Au, Au/Cu thin films: novel substrates for the formation of self-assembled monolayers. *Langmuir* 2002, 18 (14), 5529-5538.

Chapter 3 Results and Discussion

3.1 Results

Table 3. 1 Summary of silica substrates in terms of sample names, treated agents and water contact angles.

Samples	Treated agents	Water contact angle \pm SD (°)
Glass	Acetone	19.3 \pm 1.6
Prh Glass	Piranha solution	5.0 \pm 1.7
C8 Glass	$\begin{array}{c} \text{O} \text{---} \text{CH}_3 \\ \\ \text{H}_3\text{C} \text{---} \text{O} \text{---} \text{Si} \text{---} \text{CH}_2(\text{CH}_2)_6\text{CH}_3 \\ \\ \text{O} \text{---} \text{CH}_3 \end{array}$	56.6 \pm 0.5
NH2 Glass	$\begin{array}{c} \text{OCH}_3 \\ \\ \text{H}_3\text{CO} \text{---} \text{Si} \text{---} \text{CH}_2\text{CH}_2\text{CH}_2\text{NH}_2 \\ \\ \text{OCH}_3 \end{array}$	37.6 \pm 2.7
Quartz	Acetone	-
Prh Quartz	Piranha solution	-
C8 Quartz	$\begin{array}{c} \text{O} \text{---} \text{CH}_3 \\ \\ \text{H}_3\text{C} \text{---} \text{O} \text{---} \text{Si} \text{---} \text{CH}_2(\text{CH}_2)_6\text{CH}_3 \\ \\ \text{O} \text{---} \text{CH}_3 \end{array}$	-
NH2 Quartz	$\begin{array}{c} \text{OCH}_3 \\ \\ \text{H}_3\text{CO} \text{---} \text{Si} \text{---} \text{CH}_2\text{CH}_2\text{CH}_2\text{NH}_2 \\ \\ \text{OCH}_3 \end{array}$	-
CTAB Glass	$\begin{array}{c} \text{CH}_3 \text{ Br}^- \\ \\ \text{H}_3\text{C}(\text{H}_2\text{C})_{15} \text{---} \text{N}^+ \text{---} \text{CH}_3 \\ \\ \text{CH}_3 \end{array}$	35.3 \pm 2.1
PVAm (10 kDa) Glass	$\begin{array}{c} \text{---} (\text{CH} \text{---} \text{CH}_2)_n \text{---} \\ \\ \text{NH}_2 \end{array}$	35.5 \pm 2.8
PVAm (45 kDa) Glass	$\begin{array}{c} \text{---} (\text{CH} \text{---} \text{CH}_2)_n \text{---} \\ \\ \text{NH}_2 \end{array}$	39.5 \pm 1.6
PVAm (340 kDa) Glass	$\begin{array}{c} \text{---} (\text{CH} \text{---} \text{CH}_2)_n \text{---} \\ \\ \text{NH}_2 \end{array}$	45.9 \pm 2.2

PNIPAM Glass	$\begin{array}{c} \text{-(CH-CH}_2\text{)}_n \\ \\ \text{O=CHNHCH(CH}_3\text{)}_2 \end{array}$	53.1 ± 2.7
NH2-PNIPAM Glass	$\begin{array}{c} {}_2\text{HN-(CH-CH}_2\text{)}_n \\ \\ \text{O=CHNHCH(CH}_3\text{)}_2 \end{array}$	44.7 ± 1.6

Water contact angle measurements were performed on treated glass slides and the results are summarized in **Table 3.1**. The water contact angle of Prh Glass slide was significantly lower (~5°) than that of the acetone treated glass slide. Silane coupling agents increased the hydrophobicity of C8 Glass and NH2 Glass slides.

The adhesion properties of the prepared samples were monitored by 90° peel test. Peel strength was obtained by the average peel force per unit width of the bonded zone in the steady state, which was used to evaluate the adhesion between PDMS strip and respective substrate. **Figure 3.1** shows the peel strengths of PDMS films against chemical-modified glass surface. Prh Glass had highest peel strength with about 91 N/m; the peel strengths for silane coupling agents treated glass slides significantly decreased to 55 N/m for C8 Glass and 34 N/m for NH2 Glass. Similar changes were observed for quartz samples expect that C8 Quartz had lowest peel strength (**Figure 3.2**).

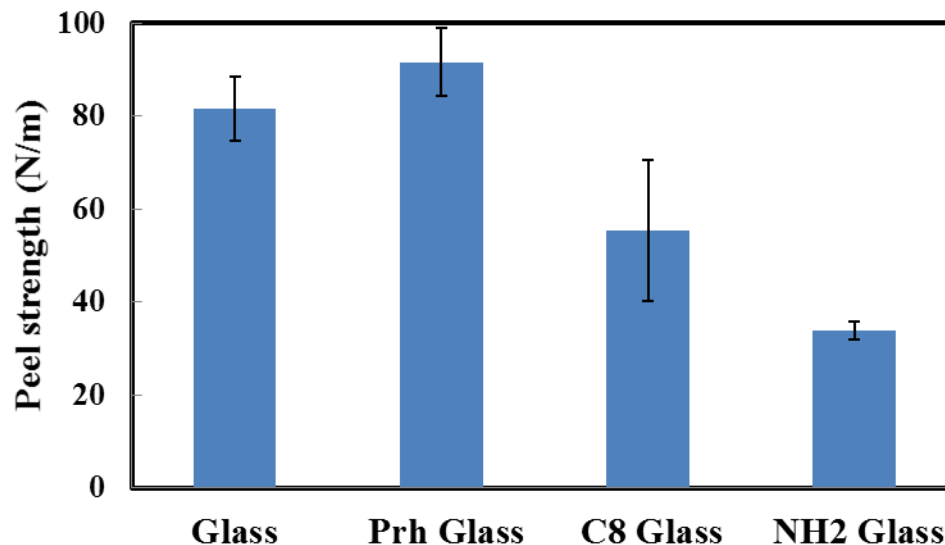


Figure 3. 1 Peel strengths of PDMS films against chemical-modified glass substrates from 90° peel tests. The peel tests were carried out with a 90° peel fixture and at a crosshead rate of 50 mm/min at 23 °C and 50% RH. The error bars represent the standard deviation of the peel strength change of four replicates.

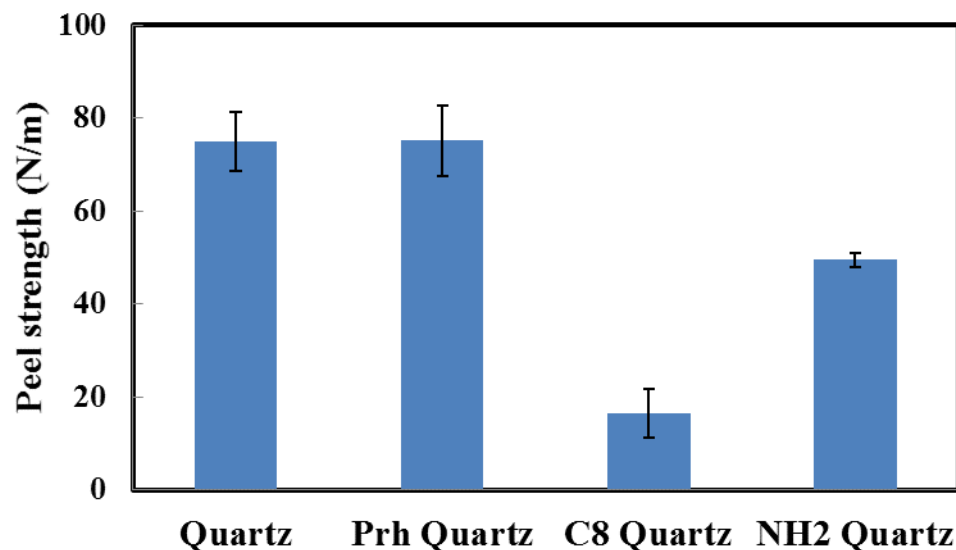


Figure 3. 2 Peel strengths of PDMS films against chemical-modified quartz substrates from 90° peel tests. The peel tests were carried out with a 90° peel fixture and at a crosshead rate of 50 mm/min at 23 °C and 50% RH. The error bars represent the standard deviation of the peel strength change of four replicates.

Figure 3.3 summarizes the peel strengths of PDMS films against physical-adsorbed glass substrates. The CTAB treated glass slide had almost the same peel strength as that without CTAB. The adsorption of water-soluble polymer onto the glass surface reduced at least 50% of the peel force against PDMS films. PNIPAM were more effective to lower the adhesion force than PVAm, and the peel force of PVAm decreased with the increasing of molecular weight.

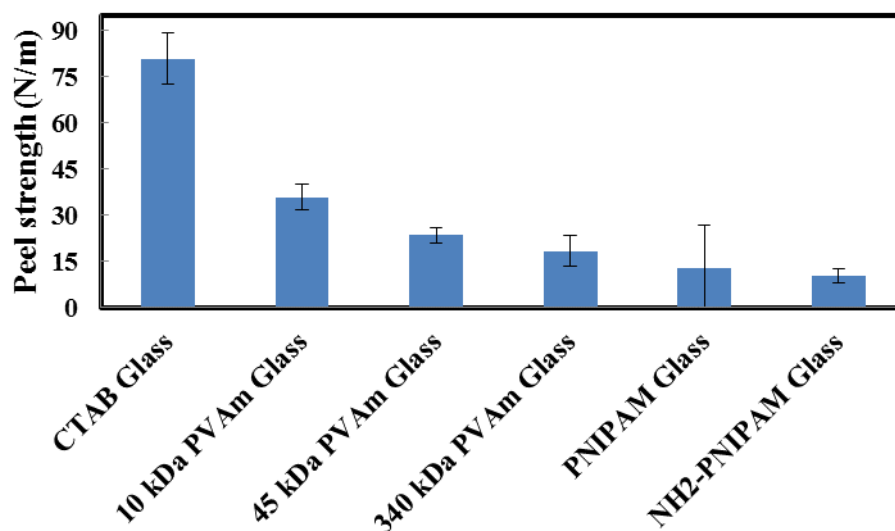


Figure 3. 3 Peel strengths of PDMS films against physical-adsorbed glass substrates from 90° peel tests. The peel tests were carried out with a 90° peel fixture and at a crosshead rate of 50 mm/min at 23 °C and 50% RH. The error bars represent the standard deviation of the peel strength change of four replicates.

In order to test the long-term lubricating properties of PVAm, new PDMS films were prepared on the peeled PVAm Glass slides. The corresponding peeling results (**Figure 3.4**) show a slight increase of peel strength for the adhesion samples with the recycled substrates, indicating that the existence of high content of PVAm on the substrate and thus maintaining good debonding performance.

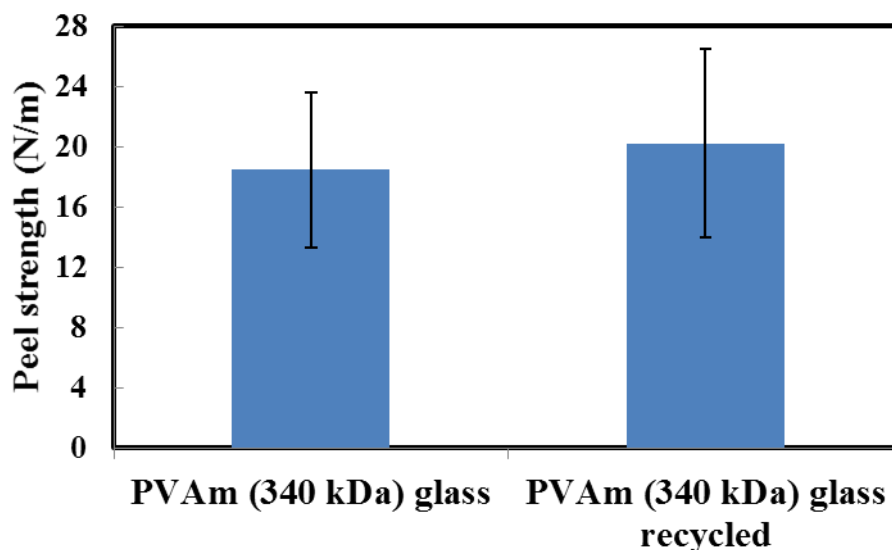


Figure 3. 4 Peel strengths of PDMS films against PVAm (340 kDa) adsorbed glass substrate and recycled PVAm (340 kDa) adsorbed glass substrate from 90° peel tests. The peel tests were carried out with a 90° peel fixture and a crosshead rate of 50 mm/min at 23 °C and 50% RH. The error bars represent the standard deviation of the peel strength change of four replicates.

Table 3.2 compares the relative atomic concentration of glass substrate surface before peel tests with those after peel tests. The relative oxygen concentration significantly decreased for all the glass substrate except NH₂ Glass substrate. Also there was about 10% carbon concentration on Piranha Glass substrate. Judging from **Table 3.3** the relative atomic concentration of nitrogen in PVAm (340 kDa) changed slightly after peel test.

Table 3. 2 Relative atomic concentration (%) of different glass substrate surfaces at 45° takeoff angle by XPS before and after PDMS peel tests.

Samples	Relative atomic concentration at 45° takeoff angle (%)									
	C		O		Na		Si		N	
	Before	After	Before	After	Before	After	Before	After	Before	After
Glass	17.89	44.26	58.54	33.25	3.18	0.62	20.39	21.87	-	-
Prh Glass	10.17	44.14	63.04	32.96	2.34	1.38	24.45	21.51	-	-
C8 Glass	21.47	37.37	52.84	40.04	3.34	1.62	21.49	20.97	-	-
NH2 Glass	49.48	44.26	27.56	31.39	-	-	13.53	20.81	9.43	3.54

Table 3. 3 Relative atomic concentration (%) of PVAm (340 kDa) adsorbed glass substrate surfaces at 45° takeoff angle by XPS before and after PDMS peel tests.

Samples	Relative atomic concentration at 45° takeoff angle (%)					
	C	N	O	Si	Na	Ca
Before peeling	26.92	5.06	46.97	19.23	0.50	0.65
After peeling	33.76	3.59	40.57	21.20	0.57	0.31

SEM imaging and optical imaging were carried out to analysis the changes of surface morphology after peel tests. As **Figure 3.5** shown there were some PDMS residues on the peeled glass substrates. Prh Glass and Glass substrates had a layer-like residues covered on the surface while C8 Glass had some small scattered residues with the size of around 1 μm . I presume that the relatively strong interactions between PDMS and glass substrate would

cause more PDMS residues. When the relatively strong adhesion force is higher than the surface strength of PDMS in the interface, PDMS laminate in the interface broke and left residues on the substrate surface. However, NH₂ Glass had some 5~10 μm large residues on the substrate.

Optical images were taken on the peeled substrates and ATR-FTIR was performed to further illustrate the chemistry of the residues. There were some residues observed for the adhesion samples Prh Glass/PDMS and Glass /PDMS in **Figure 3.6**, and not significant residues for C8 Glass/PDMS and NH₂ Glass/PDMS, which was due to the low resolution of the optical images.

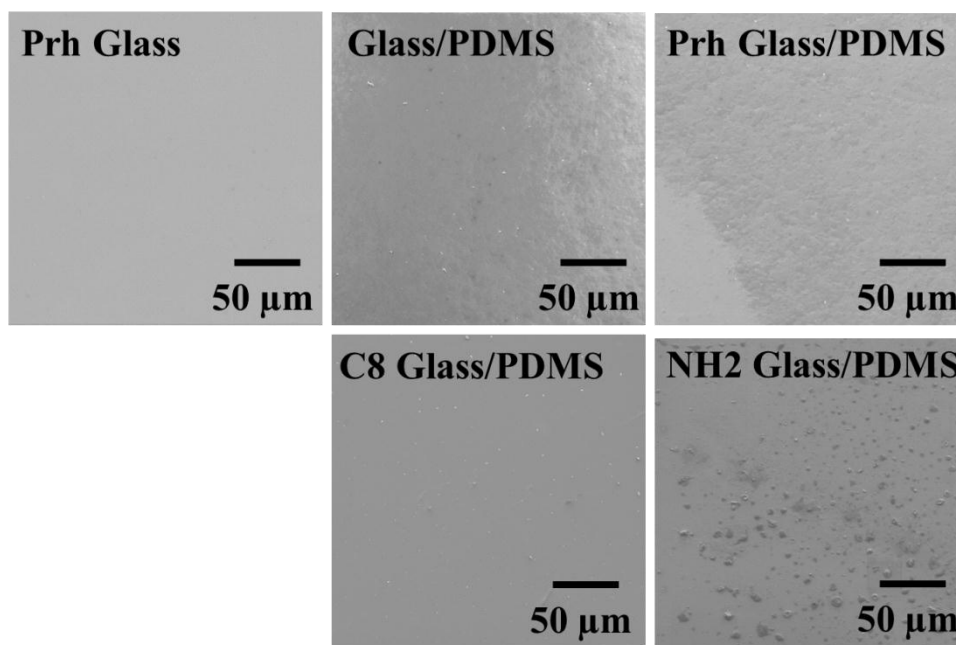


Figure 3. 5 SEM images of different chemical-modified glass substrates after 90° peel test.

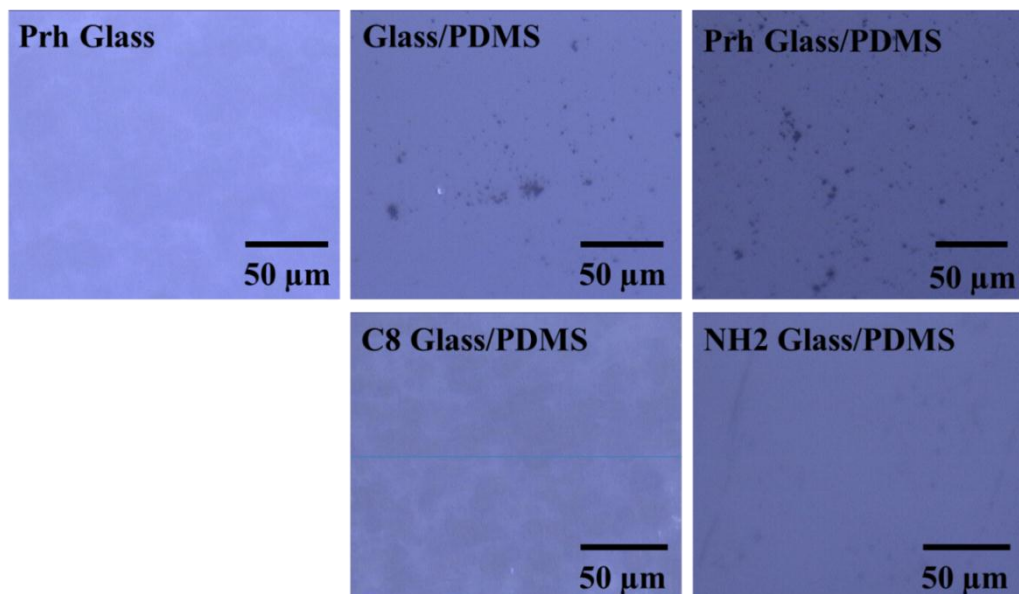


Figure 3. 6 Optical images of peeled substrate surfaces and pure Prh Glass surface as control.

Surface ATR-FTIR spectra were obtained by scanning at least three of the residue spots and averaging the signals. As shown in **Figure 3.7** the surface ATR-FTIR spectra of the peeled samples were similar for all Glass, Phr Glass, C8 Glass and NH2 Glass slides. The peak at around 1265 cm^{-1} in FTIR spectrum of peeled PDMS was corresponding to the symmetric deformation of $-\text{CH}_3$ in $-\text{Si}-\text{CH}_3$. However, there was no peak at 1265 cm^{-1} for all the peeled adhesion samples, which seems that there was not PDMS residue on the adhesion sample substrates.

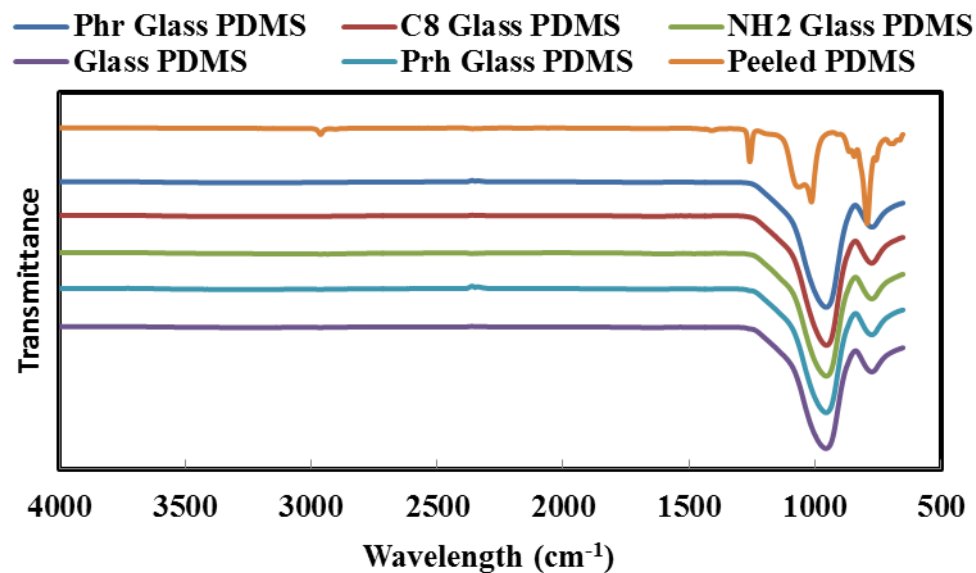


Figure 3. 7 Surface ATR-FTIR spectra of different glass substrates after peel tests.

3.2 Discussion

The adhesion between PDMS and silica substrate reflects hydrogen bond formation between oxygen in PDMS and silanol group on silica surface. **Figure 3.8** illustrates the hydrogen bonding which is considered to contribute to the strong adhesion. The adhesion force depends on the density of silanol groups on the substrate surface.

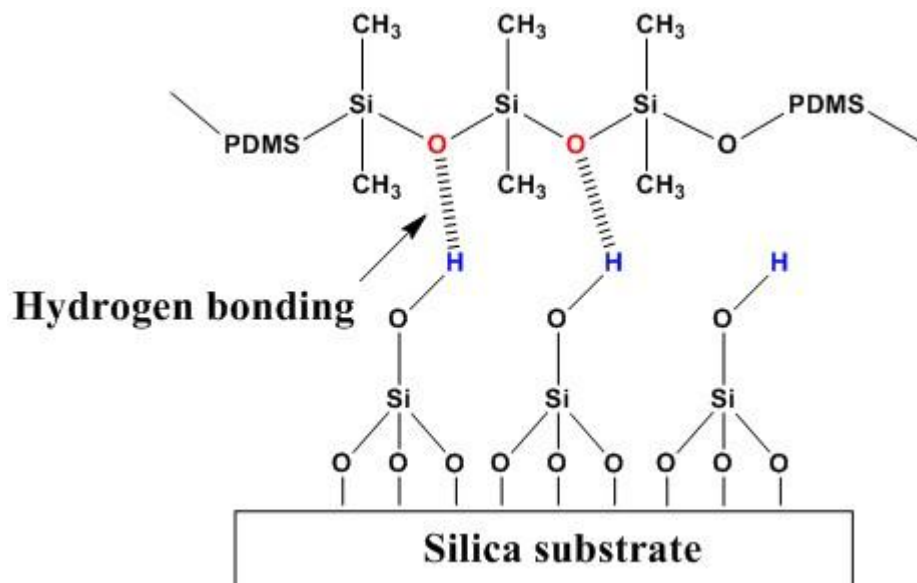


Figure 3. 8 Illustration of proposed hydrogen bonding between PDMS and silica substrate.

3.2.1 The effects of surface wettability of glass substrates on the adhesion behavior of PDMS

It is believed that good surface wettability is an important property for adhesion enhancement.^{1, 2} Water contact angle measurement is a common and direct method to evaluate the wettability of the materials surface. Lower contact angle corresponds to good surface wettability for PDMS. In my case good wettability of silica substrate promotes hydrogen bonding when PDMS comes into contact with silica substrate. **Figure 3.9** and **Figure 3.10** compares the adhesion strength with water contact angle. In **Figure 3.9** the peel strength increases with the decrease of water contact angle except for NH₂ Glass which underwent a different mechanism. There is similar trend for polymer- adsorbed substrates (**Figure 3.10**). Though CTAB adsorbed glass had similar contact angle with PVAm (10 kDa), the peel strength of CTAB was over half less than that of PVAm (10 kDa) owing to

the relative weak adsorption of CTAB and its easiness of migration to PDMS phase during thermal curing.

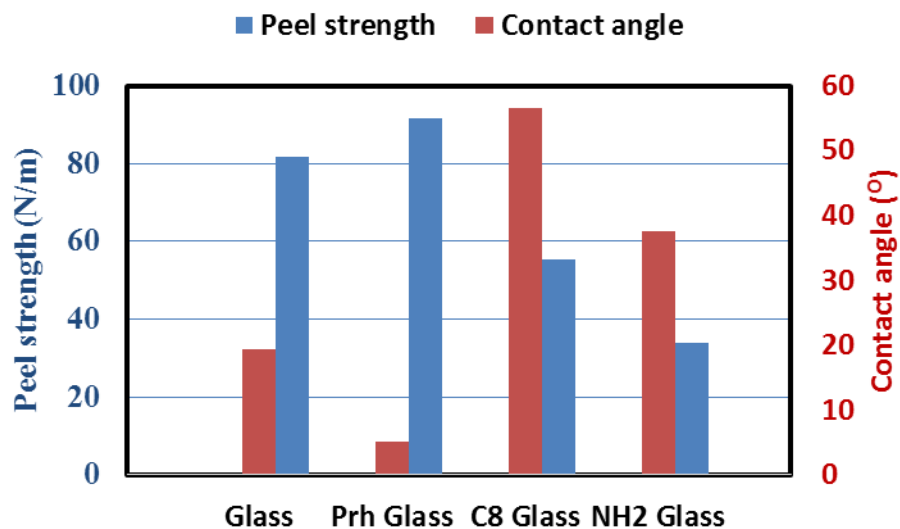


Figure 3. 9 Comparison of peel strength and contact angle for chemical-modified glass substrates.

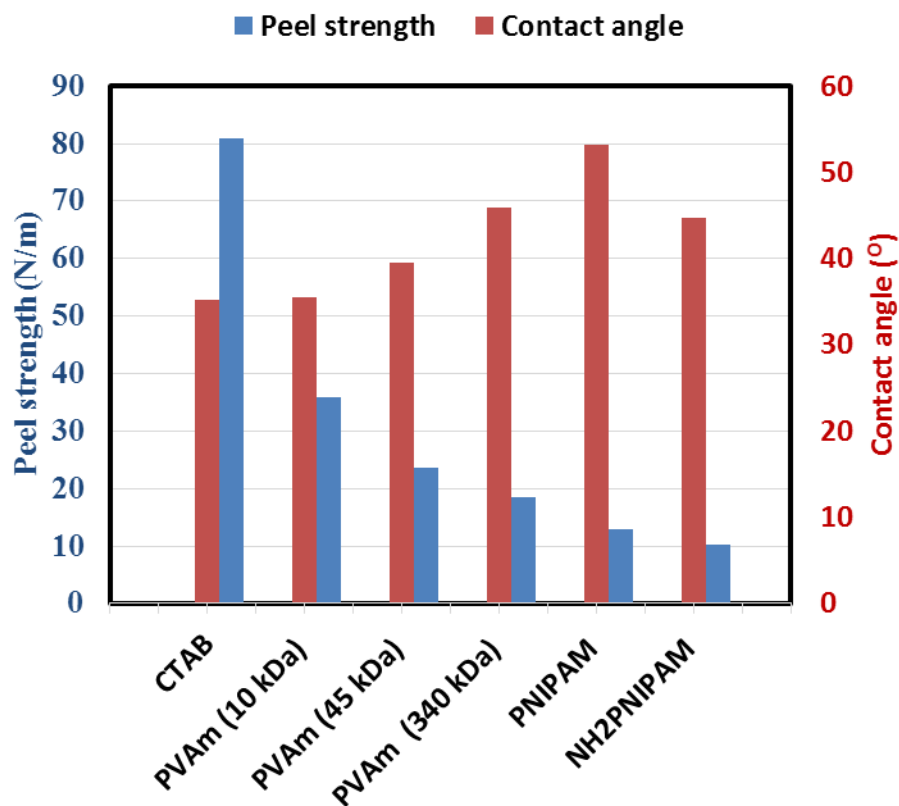


Figure 3. 10 Comparison of peel strength and contact angle for physical-adsorbed glass substrates.

3.2.2 Adhesion behavior of PDMS against glass and quartz substrates

The adhesion forces for glass and quartz based adhesion samples were compared in order to evaluate the influence of substrate compositions on the adhesion behaviors (**Figure 3.1** and **Figure 3.2**). For acetone treated and piranha solution treated glass slides they show higher adhesion force than those of quartz slides. I presumed the differences of chemical composition of glass and quartz had significant effects on the adhesion. The type of glass slides in this work was soda lime glass, comprised of 73% SiO₂, 14% Na₂O, 7% CaO, 4% MgO, 2% Al₂O₃.³ The metal oxides do not explicitly exist in glass since glass is a very complex crosslinked-like “polymer”. Prh Glass had a higher ratio of oxygen element to

silicon element than that of Prh quartz as shown in **Figure 3.11**, which indicated more hydroxyl groups on the Prh Glass surface.

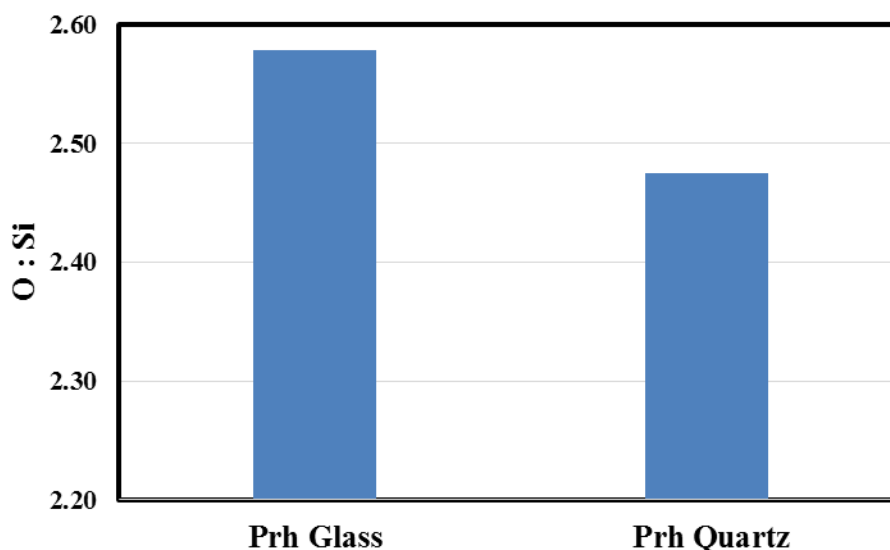


Figure 3. 11 The ratio of relative oxygen and relative silicon concentration for Prh Glass and Prh Quartz substrates.

The impurities of polar oxides in glass slides are expected to decrease the density of silanol groups and reduce the adhesion; however, glass slides had higher adhesion strength compared with quartz slides. The surface of metal oxide (eg. alumina) would easily absorb water molecule to form hydroxyl group in a moist environment,⁴ which may contribute to the relatively higher peel strength for Prh Glass substrate.

The PDMS residues on the glass substrates after peeling were analyzed to further illustrate the adhesion force by SEM imaging (**Figure 3.5**). The layer-like residues on control glass slide and piranha solution treated glass slide was due to the strong hydrogen bonding in the peel zone. The octyl chain on the C8 Glass slide significantly decreased the hydrogen

bonding, resulting small-scattered residues. Nevertheless, there were medium-size deposits on the NH₂ Glass slide where the adhesion strength was the lowest for the adhesion samples with chemical-modified glass substrates. It can be explained by the interruption of crosslinking by amino groups on the contact zone during the thermal curing process⁵. So the sticky-like residues were responsible for the lower cross-linked PDMS and even non cross-linked PDMS. There weren't apparent PDMS signals in ATR-FTIR spectra for the peeled substrates, indicating the relative small amount of PDMS residue which was consistent with the respective optical images.

3.2.3 Adhesion behavior of PDMS against chemical-modified and physical-adsorbed glass substrate

Silane coupling agents were reacted with piranha solution treated glass slides to give chemical-bonded octyl chain and amino groups on C8 Glass substrate and NH₂ Glass substrate, respectively. Hexadecyl chains were physical-adsorbed on CTAB Glass substrate. The adhesion force for CTAB Glass adhesion sample was almost the same with those of Piranha Glass, suggesting that inert CTAB had no significant effects in the adhesion zone. On one hand the adsorbed amount of CTAB on the silica substrate was relative small. On the other hand, the small molecule of CTAB was easy to migrate to PDMS prepolymer phase without inhibiting the formation of crosslinking network during thermal curing process.

The physical adsorption of water-soluble polymers as debonding agents provides a simple method to investigate the adhesion mechanism. In this work PVAm and PNIPAM were

chosen as model polymers. The adsorption of PVAm and PNIPAM on glass substrates was driven by hydrogen bonding. Compared with small molecular weight silane coupling agents and surfactant, the long chains of PVAm and PNIPAM induced denser coverage, promoting higher screening effect between PDMS and glass substrate. So it reduced the density of effective silanol groups on the substrate surface and thus decreased the formation of hydrogen bonding.

3.2.4 The effects of molecular weight of absorbed PVAm on adhesion

The molecular weight of absorbed PVAm had profound effects on reducing the adhesion force. The amount of PVAm adsorbed on glass surface is of molecular weight and degree of hydrolysis dependent, and increases significantly with increasing the molecular weight and degree of hydrolysis of PVAm, respectively.^{6,7} The greater the amount of PVAm adsorbed on glass surface the higher density of primary amino groups. The adhesion force for adhesion sample PVAm (10 kDa) was higher than that of PVAm (45 kDa) where both of their degrees of hydrolysis were about 75%. And PVAm (340 kDa) had highest molecular weight and degree of hydrolysis and thus lower adhesion force.

Primary amino groups in PVAm can poison the platinum catalyst and inhibit the crosslinking process of PDMS during thermal curing.⁵ In addition the amines groups in PNIPAM can compete for the Si-H bond and involved in undesired side reaction during the curing process.⁵ Both of the poison effect and undesired side reaction can inhibit the effective formation of crosslinked PDMS network in the interface of PDMS and silica

substrate. Ineffective crosslinked PDMS on the surface of bulk PDMS rubber had low mechanical strength, which makes the PDMS easy to be peeled off. The higher density of primary amino groups on the substrate the lower adhesion it would be.

3.3.5 The adhesion behavior of PDMS on recycled PVAm substrates

There was a slight increase of peel strength for the adhesion sample prepared on peeled PVAm (340 kDa) absorbed glass substrate, which indicated the existence of most PVAm residues remaining. In addition this explanation is supported by the XPS result illustrated in **Table 3.3**. The polar PVAm is poorly miscible with PDMS exhibiting relative phase separation in their interface, thus the migration of PVAm chain into the PDMS matrix is restricted. Then the abundant of primary amino groups still maintained the inhibition of PDMS crosslinking in the interface which reduced the adhesion force. The immiscible property of PVAm and PDMS is considered to contribute to the long-term debonding performance.

References

1. Mittal, K. L., *Contact angle, wettability and adhesion*. CRC Press: 2006; Vol. 4.
2. Good, R. J., Contact angle, wetting, and adhesion: a critical review. *Journal of adhesion science and technology* **1992**, 6 (12), 1269-1302.
3. Fillery, S. P., *Mechanics of graded glass composites and zinc oxide thin films grown at 90 degrees Celsius in water*. ProQuest: 2007.
4. Semoto, T.; Tsuji, Y.; Yoshizawa, K., Molecular Understanding of the Adhesive Force between a Metal Oxide Surface and an Epoxy Resin. *The Journal of Physical Chemistry C* **2011**, 115 (23), 11701-11708.
5. Ortiz-Acosta, D. Sylgard® Cure Inhibition Characterization; Los Alamos National Laboratory (LANL): 2012.
6. Voigt, I.; Simon, F.; Komber, H.; Jacobasch, H.-J.; Spange, S., Controlled synthesis of stable poly (vinyl formamide-co-vinyl amine)/silica hybrid particles by interfacial post-cross-linking reactions. *Colloid and Polymer Science* **2000**, 278 (1), 48-56.
7. Seifert, S.; Höhne, S.; Simon, F.; Hanzelmann, C.; Winkler, R.; Schmidt, T.; Frenzel, R.; Uhlmann, P.; Spange, S., Adsorption of Poly (vinylformamide-co-vinylamine) Polymers (PVFA-co-PVAm) on Copper. *Langmuir* **2012**, 28 (42), 14935-14943.

Chapter 4 Conclusions

The adhesion between poly(dimethyl siloxane) silicon rubber and silica substrates was studied by 90° peel tests. This work reveals that the adhesion force strongly depends on the surface chemistry of the silica substrate. The major conclusions of this work are shown as follows:

1. Generally silicone/glass adhesion reflects hydrogen bond formation between oxygen in PDMS and silanol group on silica surface supported by the peel test results and substrate surface characteristics. The adhesion force depends on the density of silanol groups on the substrate surface.
2. The adhesion can be tailored by silica surface treatment through either chemical modification with silane coupling agents or physical adsorption with water-soluble polymers. PNIPAM and PVAm are good debonding agents due to their dense coverage on the silica surface and thus screening the hydrogen bond. The coverage of PVAm increases with molecular weight and thus higher molecular weight PVAm have better debonding effects.
3. The introduction of primary amino groups onto the surface of silica substrate is gives reduced adhesion because primary amino groups can poison the catalyst during the curing of PDMS in the interface of PDMS and silica surface. The resulting PDMS with lower crosslinking in the outer surface was easy to be removed and thus having lower adhesion.
4. Judging from the XPS results there was slightly decline of PVAm (340 kDa) on the substrate after peel test, which may contribute to the relative immiscibility of

PVAm and PDMS in the peel zone. It makes PVAm a potential debonding agent for long-term application.